10-15-2007

Airway Strain during Mechanical Ventilation in an Intact Animal Model

Scott W. Sinclair
University of Tennessee Health Science Center

Robert C. Molthen
Marquette University, robert.molthen@marquette.edu

Steven Thomas Haworth
Medical College of Wisconsin

Christopher A. Dawson
Medical College of Wisconsin

Christopher M. Waters
University of Tennessee Health Science Center

Airway Strain during Mechanical Ventilation in an Intact Animal Model

Scott E. Sinclair[1,2], Robert C. Molthen[3], Steve T. Haworth[3], Christopher A. Dawson[3†], and Christopher M. Waters[1,2]

[1]Department of Medicine and [2]Department of Physiology, University of Tennessee Health Science Center, Memphis, Tennessee; and [3]Department of Medicine, Medical College of Wisconsin, Milwaukee, Wisconsin

Rationale: Mechanical ventilation with large tidal volumes causes ventilator-induced lung injury in animal models. Little direct evidence exists regarding the deformation of airways *in vivo* during mechanical ventilation, or in the presence of positive end-expiratory pressure (PEEP).
Objectives: To measure airway strain and to estimate airway wall tension during mechanical ventilation in an intact animal model.
Methods: Sprague-Dawley rats were anesthetized and mechanically ventilated with tidal volumes of 6, 12, and 25 cm^3/kg with and without 10–cm H_2O PEEP. Real-time tantalum bronchograms were obtained for each condition, using microfocal X-ray imaging. Images were used to calculate circumferential and longitudinal airway strains, and on the basis of a simplified mathematical model we estimated airway wall tensions.
Measurements and Main Results: Circumferential and longitudinal airway strains increased with increasing tidal volume. Levels of mechanical strain were heterogeneous throughout the bronchial tree. Circumferential strains were higher in smaller airways (less than 800 μm). Airway size did not influence longitudinal strain. When PEEP was applied, wall tensions increased more rapidly than did strain levels, suggesting that a "strain limit" had been reached. Airway collapse was not observed under any experimental condition.
Conclusions: Mechanical ventilation results in significant airway mechanical strain that is heterogeneously distributed in the uninjured lung. The magnitude of circumferential but not axial strain varies with airway diameter. Airways exhibit a "strain limit" above which an abrupt dramatic rise in wall tension is observed.

Keywords: airway strain; wall tension; ventilator-induced lung injury; mechanical ventilation; airway mechanics

Despite its clinical benefits, mechanical ventilation is associated with deleterious side effects. Since the pioneering report by Webb and Tierney (1) numerous studies have shown that mechanical ventilation can cause or contribute to already existing lung injury. Termed ventilator-induced lung injury (VILI), one of the prevailing mechanisms thought to be responsible for causing VILI is mechanical overdistension of the lung due to excessive tidal volumes. The impact of mechanical overdistension on patient outcomes was clearly demonstrated in a landmark study in which significantly improved mortality was observed in patients with acute respiratory distress syndrome (ARDS) and mechanically

AT A GLANCE COMMENTARY

Scientific Knowledge on the Subject

Little is known about dynamic measurements of airway strain during mechanical ventilation in intact animals.

What This Study Adds to the Field

Mechanical ventilation results in significant airway mechanical strain that is heterogeneously distributed in the uninjured lung.

ventilated with lower tidal volumes (6 cm^3/kg) compared with the standard approach (12 cm^3/kg) (2).

Another potential mechanism associated with VILI is the tidal collapse and expansion of airways and/or alveoli. This was initially hypothesized to explain the observed protective effect of positive end-expiratory pressure (PEEP) in models of VILI and postulates that large stresses are generated when airways and alveoli collapse at end exhalation and reopen during lung inflation (3–5). On the basis of these ideas, the use of PEEP has been hypothesized to protect the lung by preventing the repeated opening and closing of these regions.

Despite the substantial interest in the role of mechanical forces in VILI, there is surprisingly little direct knowledge of the localization and levels of these forces and the resultant tissue deformation. Many studies have used morphometric measurements of fixed lung tissue to assess tissue deformation as a function of lung inflation (6–10), but these techniques are limited by the potential for fixation artifacts and the use of isolated lungs. Nevertheless, these studies have raised questions about the homogeneity of deformation throughout the lung as well as the mechanisms by which deformation takes place.

Intravital microscopy has been used to visualize alveolar structures (11–16), but these techniques are also limited by the ability to visualize only subpleural structures and the invasive nature of the technique. As pointed out by Hubmayr (17), there is relatively little consensus about alveolar deformation during breathing. To extend this observation further, little direct evidence exists regarding the deformation of airways *in vivo* during mechanical ventilation, or in the presence of PEEP. In addition to the cells lining the alveolus, the epithelium of the airways is also at risk during injurious patterns of mechanical ventilation. Injury to the small airway epithelium has been documented in animal models in response to overdistension with large tidal volumes (18) as well as with mechanical ventilation with low PEEP (19, 20), presumably due to repeated collapse and reexpansion of these airways.

We used microfocal X-ray imaging of rat airways to examine mechanical strain in airways down to the terminal bronchioles. On the basis of changes in diameters and lengths of bronchial segments from two-dimensional planar images, we calculated airway strain, and we then estimated airway wall tension using

a simplified mathematical model. The goals of this study were to make dynamic measurements of the degree of mechanical strain imposed on airways during mechanical ventilation with various tidal volumes in an intact animal model, to determine how PEEP alters mechanical strain, and to determine whether or not cyclic airway collapse and expansion occurs. Some of the results of these studies have been previously reported in the form of an abstract (21).

METHODS

See the online supplement for a detailed description of methods.

Animal Preparation

Experiments were performed according to Institutional Care and Use Committee guidelines and the National Institutes of Health (Bethesda, MD) *Guide for the Care and Use of Laboratory Animals.* Five Sprague-Dawley rats were anesthetized and the trachea and carotid artery were cannulated with polyethylene tubes. Rats were placed on the object stage of a microfocal X-ray imaging system, in the right lateral decubitus position, and mechanically ventilated with a tidal volume of 6 cm^3/kg, PEEP = 5 cm H$_2$O, F$_{IO_2}$ = 0.21, and a respiratory rate that kept the Pa$_{CO_2}$ at 35–45 mm Hg. Airway pressures were continuously measured and recorded.

Microfocal X-ray Imaging

The microfocal X-ray imaging system was constructed and designed at the Zablocki VA Medical Center/Keck Functional Imaging Center (Milwaukee, WI). Details of the imaging system have been published (22, 23). Briefly, it is composed of a FEINFOCUS 100.50 X-ray source (3-μm focal spot; Comet North America, Stamford, CT), an AI-5830-HP image intensifier (North American Imaging, Camarillo, CA) coupled to a Silicon Mountain Design SMD1M-15 CCD camera (DALSA, Waterloo, ON, Canada), and a specimen micromanipulator stage (translational accuracy, 1 μm; New England Affiliated Technologies/Danaher Precision Systems, Salem, NH), all mounted on a precision rail (relative positional accuracy, 10 μm).

Airway Imaging

Tantalum dust, passed through a 5-μm filter, was injected into the ventilator circuit at the onset of inflation via a timed valve. Labeled airways were imaged during mechanical ventilation with low (LV = 6 cm^3/kg), medium (MV = 12 cm^3/kg), and high tidal volumes (HV = 25 cm^3/kg) at PEEP = 0 and 10 cm H$_2$O. Under each condition, approximately 300 images were obtained at 27 frames/second at both low and high magnification. Additional images for spatial calibration were obtained with a 2,000- and 500-μm specimen translation for each magnification, respectively. Measurements made from these images and their corresponding airway pressures were used to calculate circumferential and linear strains. Examples of the locations of measurements are shown in the online supplement (*see* Figures E1A and E1B of the online supplement). Specific landmarks were used to measure diameters and lengths at the same locations for each condition.

Airway Strain and Tension Calculations

Tissue deformation was expressed as mechanical strain. Changes in diameter or segment length were used to determine circumferential strain

$$E_\theta = (D - D_0)/D_0 \qquad (1)$$

and longitudinal strain

$$\epsilon_z = (L - L_0)/L_0 \qquad (2)$$

where D is the diameter, L is the length of a segment, and D$_0$ and L$_0$ are the initial values determined at end expiration. Custom software was used to measure diameters and lengths based on specific image landmarks. Measurements made with and without PEEP were referenced to D$_0$ values at end expiration with no PEEP.

To approximate the stress distribution in the airways, we assumed the airways to be thin-walled cylinders and followed the analysis of Powell (24) and Green and Adkins (25). The circumferential wall tension is given by

$$T_\theta = \sigma_\theta \times t_0 = (1/2)D_0 P \lambda_z \lambda_\theta^2 \qquad (3)$$

and longitudinal wall tension by

$$T_z = \sigma_z \times t_0 = (1/4)D_0 P \lambda_z \lambda_\theta^2 \qquad (4)$$

where λ_z ($\lambda_z = L/L_0$) and λ_θ ($\lambda_\theta = D/D_0$) are the principal stretch ratios, σ_θ is circumferential wall stress, σ_z is longitudinal wall stress, t_0 is wall thickness, and P is the distending pressure estimated from the difference between airway pressure and esophageal pressure. Pleural pressures were assumed to be negligible on the basis of preliminary measurements of esophageal pressure that indicated that pressure changes were small relative to the changes in airway pressure (data not shown). Also, we ignored the prestress due to tethering forces that tend to keep airways open in the intact animal and active force generated by smooth muscle.

Data Analysis

One-way repeated measures analysis of variance was used for comparison of three or more conditions. If a significant difference was detected, a Student t test with the Bonferroni correction was performed between individual conditions. Comparisons between two groups were assessed by paired t test unless the groups failed a normality test, in which case the Mann-Whitney rank sum test was used. A P value of 0.05 was the predetermined threshold for significance (SigmaStat; Jandel Scientific, San Rafael, CA).

RESULTS

See the online supplement for additional results.

The monopodial structure of the rat lung results in significantly more asymmetric branching compared with its human lung counterpart. Whereas generation number and airway diameter correlate well in the human lung (26, 27), this is not the case in rats, and previous studies suggest that airway diameter is a more informative parameter in the rat than generation number (28, 29). Therefore, the data are reported in reference to airway diameter at end exhalation rather than generation number.

Airway Strain Was Increased by Higher Tidal Volumes and PEEP

Figures 1A and 1B show low-magnification tantalum bronchogram images of a rat at end exhalation and end inspiration during spontaneous breathing. Some airways exhibited little distension during the breathing cycle, whereas other airways were substantially distended. The remaining panels (Figures 1C–1L) show higher magnification images from a different rat during mechanical ventilation with low (6 cm^3/kg), medium (12 cm^3/kg), and high (25 cm^3/kg) tidal volumes with (PEEP) and without (ZEEP) the application of 10–cm H$_2$O PEEP. The degree of mechanical distension in airways ventilated with low tidal volume was similar to that observed in rats during spontaneous breathing. Note that airway segments as small as 200 μm could be distinguished in the high-magnification images, indicating that these segments were likely near the anatomic level of the terminal bronchioles. This was supported by occasional visualization of alveolar structures. To illustrate the technique for measuring changes in distension, Figures 1K and 1L show a comparison of the diameter of one bronchial segment during medium tidal volume ventilation at end exhalation (Figure 1K) and at end inspiration without PEEP (Figure 1L). Each of the other panels (Figures 1C–1J)
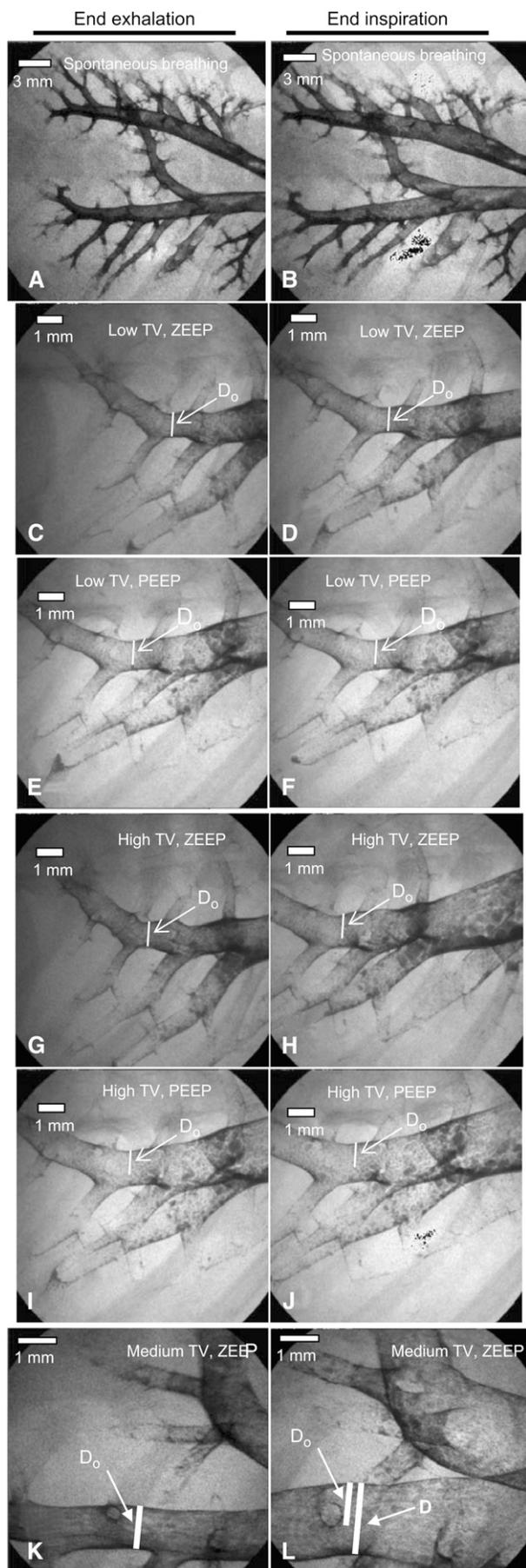
Figure 1. Tantalum bronchograms of rats during spontaneous breathing (*A* and *B*) and during mechanical ventilation with low (6 cm^3/kg; *C–F*), medium (12 ml/kg; *K* and *L*), and high (25 cm^3/kg; *G–J*) tidal volume (TV). Positive end-expiratory pressure = 10 cm H_2O (PEEP) was applied in (*E*), (*F*), (*I*), and (*J*), whereas PEEP = 0 cm H_2O (ZEEP) was applied in (*C*), (*D*), (*G*), (*H*), (*K*), and (*L*). *Left*: Images at end exhalation. *Right*: Images at end inspiration. The diameter of a single segment at end exhalation (D_0) is indicated in each of the panels (*C–J*) for comparison. (*A*) and (*B*) were obtained at low magnification (*scale bar*, 3 mm), whereas (*C*)–(*L*) were obtained at higher magnification (*scale bar*, 1 mm). (*K* and *L*) An example of the comparison between the diameter measured at end expiration (D_0) and the diameter measured at end inspiration (D) during medium tidal volume ventilation without PEEP.

contains a line indicating the diameter of a segment from that lung at end expiration without PEEP for comparison (D_0).

Measurements of circumferential airway strain as a function of airway pressure during mechanical ventilation are shown for a representative animal in Figure 2. Similar pressure–strain measurements were made for longitudinal strain, and are included in the online supplement (*see* Figure E2). Note that in this example, the circumferential strain with low tidal volume was typically less than 20% for all five segments measured, whereas strain levels with high tidal volume reached approximately 40% in each of the segments. Although the measurements from these segments are representative, there was significant heterogeneity in the levels of strain both within the same lung and in different lungs. When PEEP was applied, the level of distension at end exhalation was substantially higher in all segments, and the maximal strain levels were increased. With high tidal volume the strain levels approached 100% in this example, and even higher levels of strain were measured in other rats. (recordings of airways undergoing mechanical ventilation are available in the online supplement; *see* Videos E1 and E2).

To determine whether airway expansion occurred in an isotropic fashion, we plotted the maximal longitudinal strain versus the maximal circumferential strain for the airway segments measured from the same rat. As shown by the representative example in Figure 3, airway strain was typically anisotropic (i.e., circumferential and longitudinal strain were not equal) during mechanical ventilation. Although the application of PEEP appeared to increase circumferential strain more than longitudinal strain in this example, this was not a consistent pattern. Airway expansion was anisotropic during mechanical ventilation with each level of tidal volume, and with and without the application of PEEP.

Circumferential Strain Was Higher in Smaller Airways

To determine whether the extent of airway distension was dependent on the size of the airways, we compared the maximal strain for airways ranging in diameter from 250 to 3,000 μm at end exhalation from four different rats. Figure 4A shows that the maximal circumferential strain was higher in smaller airways when rats were ventilated with low tidal volume. As expected, the strain levels were higher with PEEP, but this did not change the general finding that higher strains were measured in smaller airways. Figure 4B shows the same comparison for rats ventilated with high tidal volume. As a further comparison, we grouped airways into two categories, either greater than (large) or less than (small) 800 μm in diameter. The 800-μm–diameter cutoff was chosen because it roughly divided the airways we were able to visualize into two equal groups. Approximately 48% of measured airways had a resting diameter above 800 μm,
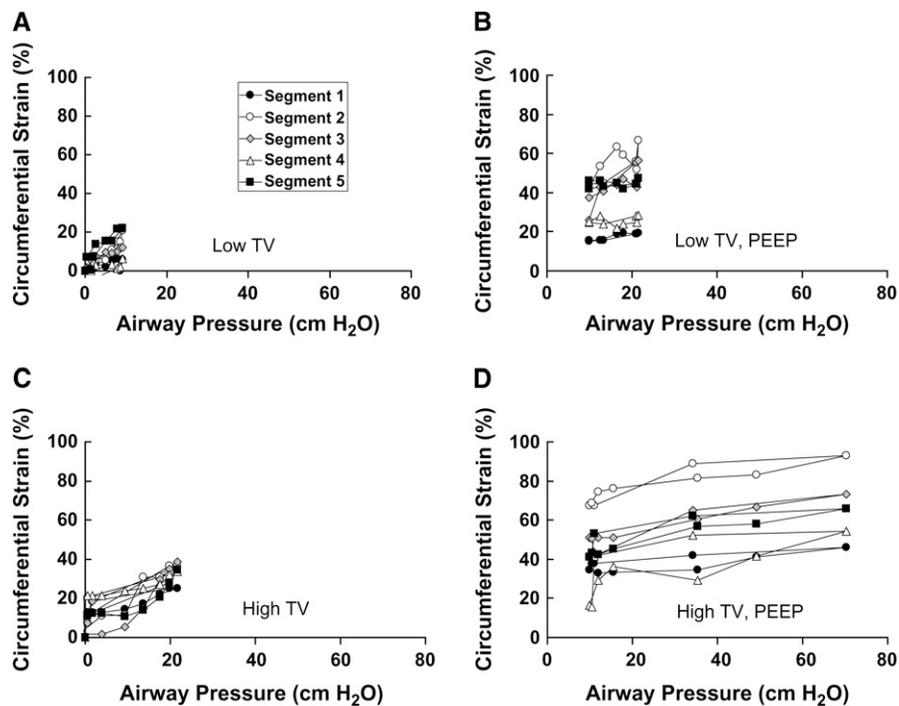
Figure 2. Circumferential strain expressed as a percentage change from end-exhalation diameter (D_0) in five different airway segments from a representative animal during mechanical ventilation with low tidal volume (6 cm³/kg) [(*A*) PEEP = 0; (*B*) PEEP = 10 cm H_2O] and high tidal volume (25 cm³/kg) ([*C*] PEEP = 0; [*D*] PEEP = 10 cm H_2O). Each curve shows the circumferential strain as a function of airway pressure for a given segment during a tidal breath (both inspiration and exhalation). Measurements shown in this figure are from low-magnification images of a representative rat with diameters of the measured segments as follows: segment 1, 1,990 μm; segment 2, 1,470 μm; segment 3, 1,150 μm; segment 4, 1,110 μm; and segment 5, 1,640 μm. TV = tidal volume.

whereas the remaining 52% had diameters below this threshold. In the animals we studied, the airways greater than 800 μm were, on average, confined to the first seven or eight airway generations. The maximal circumferential strain was significantly higher when PEEP was applied at all levels of tidal volume and in both small and large airways (Figure 4C). When comparing small and large airways, the maximal circumferential strain was significantly higher in small airways with all levels of tidal volume in the absence of PEEP. In rats ventilated with PEEP, circumferential strain levels were significantly higher in smaller airways with both medium and high tidal volumes compared with low tidal volumes, but there was no significant difference between medium and high tidal volume circumferential strain. When we compared maximal longitudinal strain in the absence of PEEP, high tidal volumes produced significantly increased strain compared with low tidal volume ventilation. Although there was a trend toward increasing longitudinal strain with higher tidal volumes, no statistically significant difference was observed between longitudinal strain with medium and high tidal volumes (Figure 4D). Interestingly, there were no significant differences in longitudinal strain associated with airway size.

PEEP Reduced the Change in Strain during a Tidal Breath

The application of 10–cm H_2O PEEP during mechanical ventilation, as expected, kept airways distended at end exhalation and thus raised the level of maximal strain under all conditions (*see* Figures 2B and 2D). Interestingly, the pressure–strain curves showed a relatively flat strain response to tidal inflation with the application of PEEP, even with larger tidal volumes. We therefore examined the maximal change in airway strain that occurred during a given tidal volume (termed "intratidal strain") in the presence and absence of PEEP. In the absence of PEEP, longitudinal intratidal strain was significantly increased in both small and large airways with increasing tidal volume (Figure 5A). For each tidal volume tested, the application of PEEP significantly decreased longitudinal intratidal strain in the large airways (Figure 5B). A similar trend was seen in the small airways but this did not reach statistical significance.

The effect of PEEP on circumferential intratidal strain was more complex (Figure 5B). Circumferential intratidal strain was significantly increased with both medium and high tidal volumes in the absence of PEEP. In large airways (diameter exceeding 800 μm) ventilated with medium and high tidal volumes, PEEP significantly reduced intratidal circumferential strain much like that observed with longitudinal intratidal strain. However, when airways with an end-exhalation diameter less than 800 μm were compared, intratidal strain increased with increasing tidal volume regardless of the presence or absence of PEEP, and circumferential intratidal strains were consistently larger in the smaller airways, regardless of condition.

Relationship between Airway Strain and Wall Tension during Mechanical Ventilation

Because there is currently substantial interest in how the levels of mechanical forces change during mechanical ventilation and how these changes may impact lung injury and repair, we developed an approach to estimate airway wall tension as a function of airway strain under different conditions. The measurements of strain discussed above directly reflect the longitudinal or circumferential deformations of the airway wall. *Stress* is a measure of the force per unit area distributed within the airway wall due to the distending pressure. Stress–strain relationships are often used to describe the mechanical behavior of materials, but we were limited in our approach because we did not have an independent measure of airway thickness. Therefore, on the basis of independent measurements of distending pressure and longitudinal and circumferential strain, we estimated airway wall *tension* (force per unit length), which is equivalent to stress × wall thickness (*see* Methods). Figure 6 shows plots of longitudinal airway wall tension versus longitudinal strain for a representative animal. With low tidal volume in the absence of PEEP, the tension–strain profile differs for each airway, but in general, the strain continues to increase throughout the tidal breath (Figure 6A). Although the levels of strain and tension were increased with high tidal volume, similar tension–strain profiles were observed (Figure 6C). When PEEP was applied in each case, the tension levels increased more rapidly than the strain levels, suggesting that a "strain
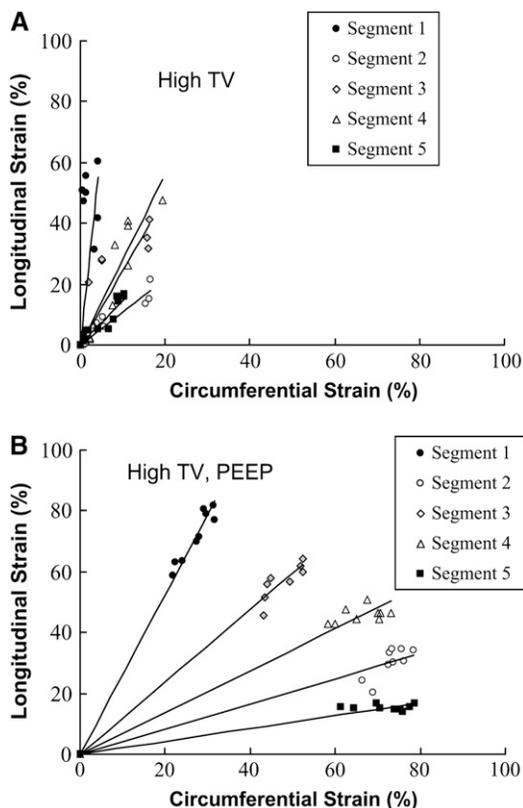
Figure 3. Airway strain was anisotropic. Shown is the relationship between longitudinal and circumferential strain in five different airways from a representative animal during mechanical ventilation with high tidal volume (25 cm³/kg) in the absence (*A*) and presence (*B*) of 10 cm H₂O positive end-expiratory pressure (PEEP). The *lines* indicate the best-fit line (forced through the origin) for the strain measurements in a given segment. Comparisons in this figure are from the same segments as in Figure 2. TV = tidal volume.

limit" had been reached (Figures 6B and 6D). Similar tension–strain profiles were obtained for circumferential measurements.

Airway Collapse Was Not Observed

We did not observe collapse of airways in any of the animals ventilated with the different tidal volumes with or without PEEP, but these animals did not have existing lung injury. The smallest airways observed were 200–300 μm, so it is possible that collapse occurred but was not visible. We were able to induce airway collapse by applying a negative airway pressure as shown in Figure 7.

DISCUSSION

We have demonstrated a method that allows real-time measurements of airway strain and simplified estimations of wall tension during mechanical ventilation in a living animal model. The principal findings of this study are as follows: (*1*) airway strain is heterogeneous and anisotropic; (*2*) circumferential strains are greater in smaller airways (less than 800 μm in diameter), but airway size does not influence longitudinal strain; (*3*) PEEP significantly reduces intratidal strain except in the case of circumferential strain in smaller airways; and (*4*) airways exhibit an apparent "strain limit" above which airway tensions increase dramatically while strain levels plateau.

Limitations of the Experimental Model

The principal limitation of this study was the inability to consistently image and measure strain in alveolar structures. We recognize the importance of measuring the mechanical forces experienced at the alveolar level in the understanding of VILI, and efforts to improve image resolution in this model are ongoing. However, because VILI and ARDS also produce injury in the airway epithelium, the quantification of mechanical forces experienced in the bronchial tree during mechanical ventilation is also vital to our understanding of these diseases. One study (30) has shown that alveolar as well as distal airway injury occurs in a surfactant-depleted rat model of large tidal volume–induced lung injury and that the distributions of these two types of injury differ. Although alveolar injury was found to occur only in nondependent areas of nonatelectatic lung, distal airway injury occurred in both atelectatic and nonatelectatic lung. This finding suggests that VILI causes lung injury in both the alveoli and small airways, possibly through different mechanisms. Furthermore, changes observed in small airways in our model may be indicative of changes at the alveolar level.

Because we employ a two-dimensional planar imaging system, if an airway moves in and out of the imaging plane during a breath, the measured strain level could be altered; specifically, longitudinal strains would be underestimated. To limit this possibility, we prospectively chose to measure airways that visually appeared to remain in the imaging plane throughout the respiratory cycle. Circumferential airway measurements should not be affected. Another potential concern is that airway deformation might occur in a nonuniform/noncircular manner. However, we frequently visualized airways in cross-section, and we did not observe such noncircular deformation except when we applied the negative vacuum pressure (Figure 7). These potential limitations could be addressed by computed tomography, but this approach limits our ability to acquire images during respiratory movement.

As described in METHODS, we approximated the stress distribution in the airways by assuming the airways to be thin-walled cylinders and followed the analysis of Powell (24) and Green and Adkins (25). This assumption is valid when $(D_0/2)/t_0 > 1$, where t_0 is the thickness of the airway wall at the baseline diameter D_0. According to measurements made by Powell in isolated dog lungs (24), this ratio is typically greater than 6, validating the thin wall assumption. We can define the principal stretch ratios for changes in length ($\lambda_z = L/L_0$), circumference ($\lambda_\theta = D/D_0$), and thickness ($\lambda_t = t/t_0$), and due to incompressibility, $\lambda_z\lambda_\theta\lambda_t = 1$. Because the elongation ratios are large in the airways we could not use linearized, small strain theory of elasticity to determine mechanical relationships. Green and Adkins (25) developed nonlinear theory for this situation, and Powell (24) related this to the airways to determine the circumferential wall stress, σ_θ, and the longitudinal wall stress, σ_z. Because we did not have independent measures of wall thickness, t_0, we estimated wall tension as the product of wall stress, σ, and thickness. A limitation of this analysis is the assumption of tubes with capped ends in the calculation of wall tension. The bronchial segments in an intact lung are clearly not capped, but we chose not to analyze the segments as open-ended tubes to take into account the stabilizing mechanical influence of adjacent airways and prestress due to tethering forces that tend to keep airways open. We also ignored changes in pleural pressures (estimated by esophageal pressures in preliminary experiments) and active force generated by smooth muscle. These assumptions were made to simplify the analysis of airway wall stress because we do not have independent measurements of tethering forces or smooth muscle tension. By ignoring these factors, we
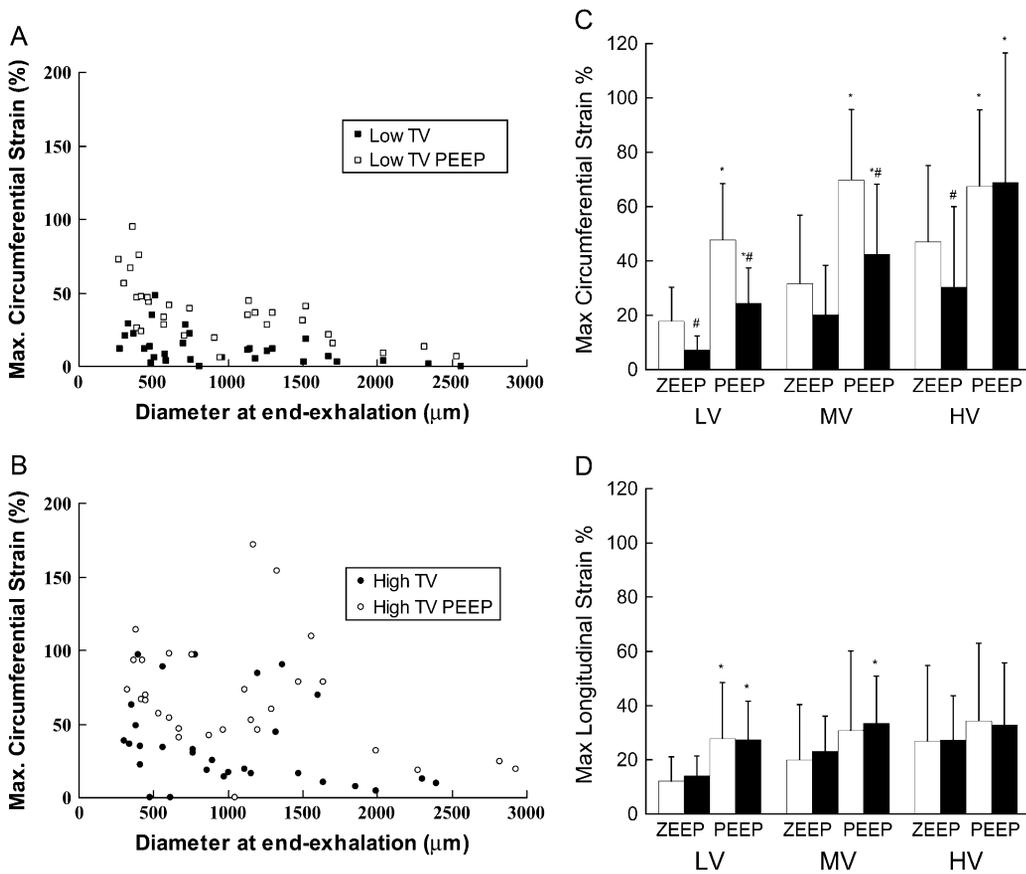
Figure 4. Maximal strain levels were dependent on tidal volume, positive end-expiratory pressure (PEEP), and airway size. (*A*) Maximal circumferential strains measured during low tidal volume mechanical ventilation (6 cm^3/kg) as a function of airway diameter at end exhalation from four different rats. (*B*) Strains generated by high tidal volume ventilation (25 cm^3/kg). In both (*A*) and (*B*), *solid symbols* represent measurements made with PEEP = 0 whereas *open symbols* represent measurements made with PEEP = 10 cm H$_2$O. (*C* and *D*) Overall effect of the three experimental tidal volumes with and without PEEP on maximal circumferential (*C*) and longitudinal (*D*) strain. *Solid symbols* indicate mean values for airways greater than 800 μm in end-exhalation diameter, whereas *open symbols* indicate mean values for airways with less than the 800-μm end-exhalation diameter. Values are reported as means ± SD. *$P <$ 0.05 when PEEP is compared with ZEEP in airways in the same airways size group; #$P <$ 0.05 when large-diameter airways are compared with small-diameter airways for each experimental condition. (*C*) All other comparisons between conditions reached statistical significance ($P <$ 0.05) except (*1*) small airways: LVZ versus MVZ, MVP versus HVP, and MVZ versus HVZ; and (*2*) large airways: LVZ versus MVZ, MVZ versus HVZ, and LVP versus MVP. (*D*) Only the following additional comparisons reached statistical significance: (*1*) small airways: HVZ versus LVZ; and (*2*) large airways: HVZ versus LVZ. No small-versus-large airway comparisons reached statistical significance. Measurements were made from five airways segments from each of four different rats. LVZ, MVZ, and HVZ = low, medium, and high tidal volume, respectively, at ZEEP; LVP, MVP, and HVP = low, medium, and high tidal volume, respectively, at PEEP.

are likely underestimating the airway wall tension because we are attributing the measured changes in dimensions solely to the distending pressure, which is also underestimated. However, despite these limitations the estimations of airway wall tension as a function of tidal volume and PEEP help to identify the strain limit observed.

Comparison with Previously Published Data

The majority of past studies have suggested that changes in lung volume are associated with isotropic alveolar expansion and contraction, and early estimates of linear mechanical strain in tissue, up to 80%, were made on the basis of changes in lung volume (31). Using tantalum dust and X-ray imaging of isolated dog lungs, measurements of changes in lengths and diameters of bronchial segments were found to correlate well with changes in the cube root of lung volume (32). In a later study, Lambert and collaborators developed a computational model to predict pressure–flow relationships in the bronchial tree based on assumptions of airway mechanical properties (33, 34). They found that predicted relationships more closely matched experimental data if changes in airway dimensions for large airways were scaled according to changes in lung volume to the one-third power, whereas smaller peripheral airways were presumed to be more compliant. This assumption is consistent with our measurements that demonstrate larger changes in airway dimensions in smaller airways. Other investigators have used tantalum

bronchograms to image airway reopening in isolated rat lungs after induced airway collapse (35), or high-resolution computed tomography to examine changes in airway diameters in dogs in response to lung inflation, breath holding, and bronchoconstriction (36–39). As mentioned above, morphometric measurement of fixed lung tissue after lung inflation is a useful approach, but this technique is limited by the potential for fixation artifacts and by the use of isolated lung models (6–10). Although the focus of our studies was on changes in airways during mechanical ventilation, our approach may also be useful for identifying regional variations in bronchial responsiveness in an intact animal.

Mucosal folding patterns observed in fixed tissue of bronchoconstricted airways have been used to suggest changes in the stiffness of asthmatic airways (40) and the presence of significant compressive stresses on the airway epithelium (41). Other studies have demonstrated that the degree of epithelial stretching and unfolding and alveolar septal unfolding were highly dependent on the lung volume history before fixation (6, 9). Tschumperlin and Margulies, using rat lungs volume cycled before fixation, demonstrated that epithelial basement membrane surface area changed little during low lung volume expansion, but changed significantly (about 40%) during high lung volume expansion (42). To avoid potential artifacts due to fixation, intravital microscopy has been used to visualize recruitment and derecruitment of alveolar structures in dog lungs (12). This technique also has limitations because only subpleural structures are visualized, and the technique is highly invasive. Nevertheless, this
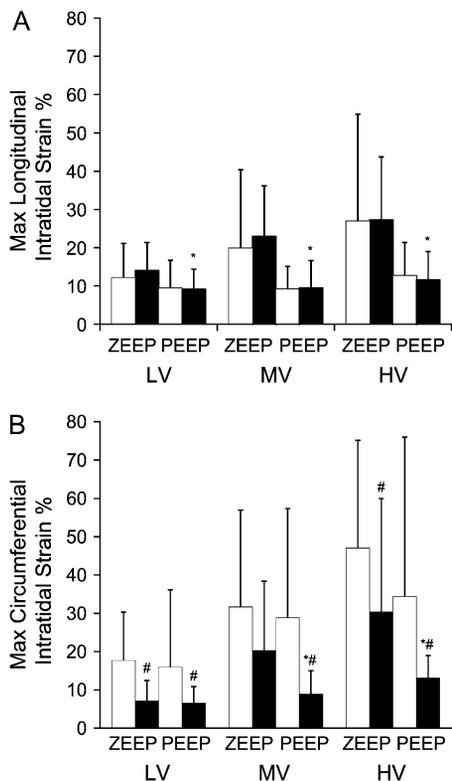
Figure 5. Changes in strain levels during a tidal breath (intratidal strain) were dependent on tidal volume, positive end-expiratory pressure (PEEP), and airway size. (*A* and *B*) Overall effect of the three experimental tidal volumes with and without PEEP on maximal longitudinal (*A*) and circumferential (*B*) intratidal strain. *Solid columns* represent large airways (end-exhalation diameter, greater than 800 μm), and *open columns* represent small airways (end-exhalation diameter, less than 800 μm). Values are reported as means ± SD. *$P <$ 0.05 when PEEP is compared with ZEEP in airways in the same airways size group; #$P <$ 0.05 when large-diameter airways are compared with small-diameter airways for each experimental condition. (*A*) No other comparisons reached statistical significance except (*1*) small airways: LVZ versus HVZ and (*2*) large airways: LVZ versus HVZ. No small- versus large-airway comparisons reached statistical significance. (*B*) Only the following additional comparisons reached statistical significance: (*1*) small airways: LVZ versus HVZ and (*2*) large airways: LVZ versus MVZ, LVZ versus HVZ, and LVP versus HVP. Measurements were made from five airways segments from each of four different rats. LVZ, MVZ, and HVZ = low, medium, and high tidal volume, respectively, at ZEEP; LVP, MVP, and HVP = low, medium, and high tidal volume, respectively, at PEEP.

group found little change in the volume of individual alveoli during lung expansion from 20 to 80% TLC, in general agreement with Tschumperlin and Margulies (42). More importantly, however, other studies by this group using this technique have suggested that although some recruitment may occur during lung expansion at low volumes in normal lungs, alveolar overdistension does occur in injured lungs (43–46). This is consistent with our view that lung injury may lead to substantial changes in the levels of mechanical strain in the airways and alveoli. Further evidence of alveolar distension *in vivo* comes from a study using confocal fluorescence microscopy to measure plasma membrane stress failure in subpleural rat alveoli (47). Such stress failure will occur only if the cells undergo large deformations, and a significantly higher level of stress failure was observed in lungs ventilated with high tidal volume.

In the current study, we demonstrate that the circumferential and longitudinal strains experienced by airways as small as 250 μm in diameter are anisotropic and increase with increasing tidal volume and the application of PEEP. Although we were not able to reliably visualize alveoli, airway size did influence the mechanical behavior of airways during mechanical ventilation.

The Effect of Tidal Volume and PEEP: Implications for VILI

We did not observe definitive airway collapse and reexpansion in any of the animals under any of the ventilation conditions. This does not exclude such phenomena occurring in airways or alveolar structures that are smaller than the detection limit of this technique. Unstable alveolar structures that collapse and reexpand during mechanical inflation have been reported using intravital microscopic techniques, but these are seen only in injured, edematous lungs and only allow visualization of subpleural alveoli held against a microscope stage by suction. If airways do not collapse and reexpand, then explaining the protective effect of PEEP in VILI becomes more difficult and speculative. Our data would suggest that perhaps limiting the intratidal strain that occurs during mechanical ventilation might minimize the mechanical insult, thereby limiting either direct tissue injury or elaboration of inflammatory or proapoptotic mediators that would otherwise lead to lung injury. It might also be postulated from these data that change in strain during a given breath is more important in the genesis of VILI than the absolute magnitude of wall tension.

The effect of PEEP on airway strain was also dependent on airway size. We found that although longitudinal intratidal strain was limited regardless of airway diameter, circumferential intratidal strain was not reduced with the application of PEEP in airways smaller than 800 μm in diameter. This implies that the tidal volume change that occurs in the presence of PEEP is primarily changing circumferential diameter in smaller airways and perhaps alveolar structures. These airways have less rigid structural wall elements that may account for their increased compliance and ability to function as a "volume or strain capacitor" at higher airway pressures. That is to say that with the application of PEEP, as tidal volumes are increased, an increasing portion of the volume change for a given breath will be reflected to the more distal lung structures where this "strain limit" was not seen under the experimental conditions in this study. The alveoli have even less rigid supporting structures, consisting only of a dense network of capillaries embedded in a thin layer of connective tissue interstitium. Therefore, these more distal structures will be less likely to exhibit a strain limit than their more proximal larger airway counterparts. This may explain why, in models of VILI, PEEP tends to exert a protective effect when ventilation is limited to a maximal peak airway pressure (tidal volumes are lower when PEEP applied), whereas PEEP tends not to be protective when tidal volumes are kept constant (48). The strain limit observed in this study could also be an indicator of a pressure–volume threshold for VILI formation (48–50). Because we did not allow the animals to develop VILI at any given ventilator setting, we could not determine whether a traumatic strain range for the airways exists or what its magnitude might be. Given the heterogeneity of the airway strains we measured, a traumatic strain range, if it exists, would likely be different for different airways and could depend on airway size, location, path length, and so on. This question requires further investigation. Conversely, the observed strain limit may function as a protective mechanism that allows the larger conducting airways to endure significant pressure fluctuations without significant damage to its epithelial lining cells and supporting structures.

Given that airway cartilage content generally decreases with increasing distance down the airways, one could postulate that
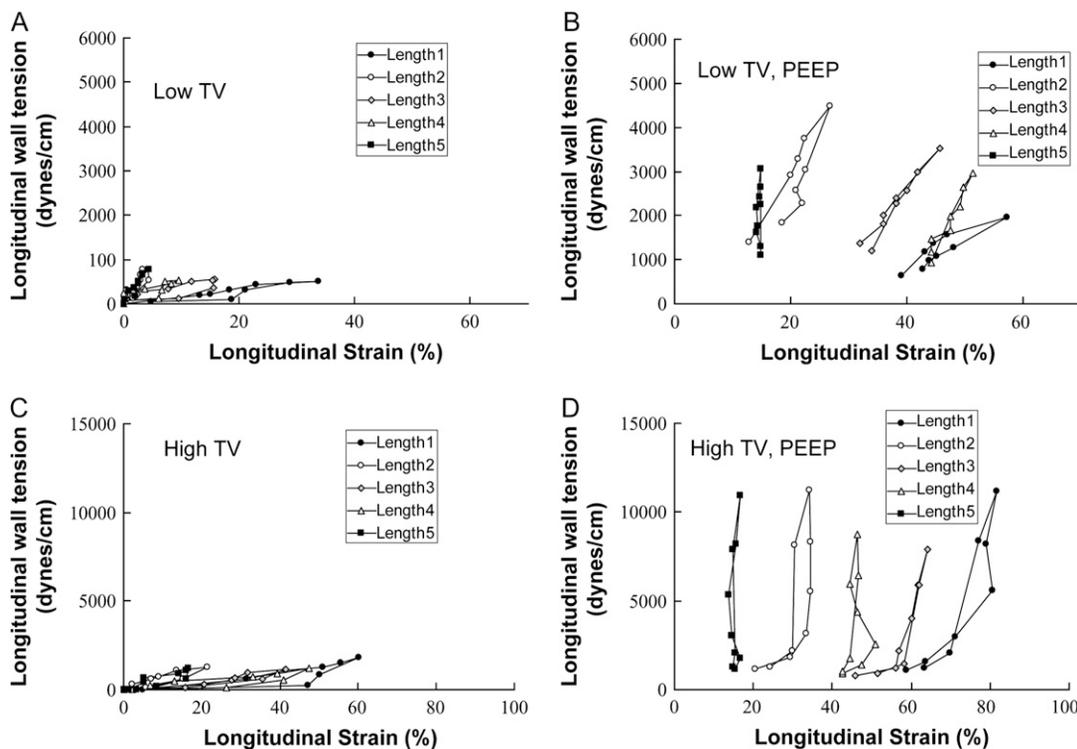
Figure 6. The relationship between longitudinal strain and airway wall tension at a given airway pressure in five different airways segments from a representative animal. (*A*) and (*B*) show this relationship during low tidal volume (6 cm³/kg) mechanical ventilation in the absence (*A*) and presence (*B*) of 10–cm H₂O positive end-expiratory pressure (PEEP). Similarly, the effects of high tidal volume ventilation (25 cm³/kg) are shown with (*C*) and without (*D*) PEEP. Comparisons in this figure are from the same segments as in Figure 2. Measurements from low-magnification images, where larger airways were measured, are shown to illustrate the strain limit seen in larger airways (greater than 800 μm) that was not evident in smaller airways (less than 800 μm). TV = tidal volume.

airway cartilage content might account for these observed strain differences in smaller airways. In isolated porcine airways subjected to bronchoconstriction by maximal electrical field stimulation or acetylcholine, airway compliance was inversely correlated to airway cartilage content (51). However, we did not measure airway cartilage content or distribution in this study, nor were we able to find quantitative morphometric data in the literature that describe the rat airway in sufficient detail to allow definitive comparisons of airway strain measurements made in the current study with airway cartilage distribution. The larger airways in our study (exceeding 800 μm) were typically found in earlier generations (those before generation 8).

In addition to the potential implications for VILI, these data may also offer insights into other pulmonary diseases, particularly those that involve primarily the airways, such as asthma. This *in vivo* airway-imaging model could be adapted to investigate the mechanical properties and behavior of airways in experimental models of asthma and bronchoconstriction. For example, a previous study by Wagers and coworkers used both experimen-

tal data and a mathematical model to predict that airway hyper-responsiveness in an allergic mouse model could be explained by thickening of the airway mucosa, but an assumption of the model was that the airways were rigid in terms of their effect on impedance (52). Our experimental results provide both anatomical information and localized compliance measurements that would enhance such an approach. In addition, our data indicating heterogeneous levels of strain and airway wall tension might be useful for modeling studies, such as those by Gillis and Lutchen (53), that predict that airway hyperresponsiveness in asthma may be due to the heterogeneity of airway wall properties. In addition, the techniques used in the current study could help to better understand airway remodeling as well as the developing lung that is subjected to mechanical ventilation.

Conclusions

In this study, we have shown the ability to measure the real-time mechanical strains and tensions experienced by the airways of an intact, living rat during mechanical ventilation under various tidal volumes with and without PEEP. Our findings suggest that a strain limit exists in the larger airways that likely reflects their mechanical properties compared with smaller airways, the walls of which are more compliant. Airway collapse and reexpansion were not observed, but a model with greater resolution or an injured lung model may be required to observe this phenomenon without the application of negative airway pressures. The application of PEEP tended to reduce intratidal strain, which may reflect the effect of PEEP on VILI, but this will require further study.

Figure 7. Tantalum bronchograms of rat airways at end exhalation (*left*) and after the application of an airway pressure of –20 cm H₂O (*right*). Negative airway pressure produces airway collapse (*right*).

References

1. Webb HH, Tierney DF. Experimental pulmonary edema due to intermittent positive pressure ventilation with high inflation pressures:
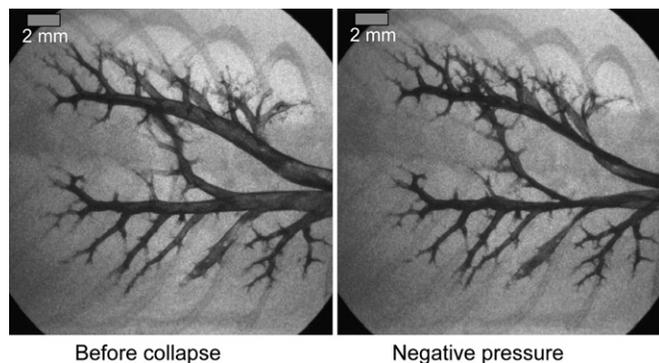
protection by positive end-expiratory pressure. *Am Rev Respir Dis* 1974;
110:556–565.

2. Acute Respiratory Distress Syndrome Network. Ventilation with lower
tidal volumes as compared with traditional tidal volumes for acute
lung injury and the acute respiratory distress syndrome. *N Engl J Med*
2000;342:1301–1308.

3. Bilek AM, Dee KC, Gaver DP III. Mechanisms of surface-tension–
induced epithelial cell damage in a model of pulmonary airway reopening.
J Appl Physiol 2003;94:770–783.

4. Kay SS, Bilek AM, Dee KC, Gaver DP III. Pressure gradient, not
exposure duration, determines the extent of epithelial cell damage in
a model of pulmonary airway reopening. *J Appl Physiol* 2004;97:269–
276.

5. Perun ML, Gaver DP III. An experimental model investigation of the
opening of a collapsed untethered pulmonary airway. *J Biomech Eng*
1995;117:245–253.

6. Bachofen H, Schurch S, Urbinelli M, Weibel ER. Relations among al-
veolar surface tension, surface area, volume, and recoil pressure. *J Appl
Physiol* 1987;62:1878–1887.

7. Gil J, Bachofen H, Gehr P, Weibel ER. Alveolar volume–surface area
relation in air- and saline-filled lungs fixed by vascular perfusion. *J Appl
Physiol* 1979;47:990–1001.

8. Gil J, Weibel ER. Morphological study of pressure–volume hysteresis
in rat lungs fixed by vascular perfusion. *Respir Physiol* 1972;15:190–
213.

9. Oldmixon EH, Hoppin FG Jr. Alveolar septal folding and lung inflation
history. *J Appl Physiol* 1991;71:2369–2379.

10. Tschumperlin DJ, Margulies SS. Alveolar epithelial surface area–volume
relationship in isolated rat lungs. *J Appl Physiol* 1999;86:026–2033.

11. Ashino Y, Ying X, Dobbs LG, Bhattacharya J. $[Ca^{2+}]_i$ oscillations reg-
ulate type II cell exocytosis in the pulmonary alveolus. *Am J Physiol
Lung Cell Mol Physiol* 2000;279:L5–L13.

12. Carney DE, Bredenberg CE, Schiller HJ, Picone AL, McCann UG,
Gatto LA, Bailey G, Fillinger M, Nieman GF. The mechanism of lung
volume change during mechanical ventilation. *Am J Respir Crit Care
Med* 1999;160:1697–1702.

13. Kuebler WM, Parthasarathi K, Wang PM, Bhattacharya J. A novel
signaling mechanism between gas and blood compartments of the
lung. *J Clin Invest* 2000;106:607.

14. Kuebler WM, Ying X, Bhattacharya J. Pressure-induced endothelial
Ca^{2+} oscillations in lung capillaries. *Am J Physiol Lung Cell Mol
Physiol* 2002;282:L917–L923.

15. Kuebler WM, Ying X, Singh B, Issekutz AC, Bhattacharya J. Pressure
is proinflammatory in lung venular capillaries. *J Clin Invest* 1999;104:
495–502.

16. Ying X, Minamiya Y, Fu C, Bhattacharya J. Ca^{2+} waves in lung
capillary endothelium. *Circ Res* 1996;79:898–908.

17. Hubmayr RD. Perspective on lung injury and recruitment: a skeptical look
at the opening and collapse story. *Am J Respir Crit Care Med* 2002;
165:1647–1653.

18. Frank JA, Gutierrez JA, Jones KD, Allen L, Dobbs L, Matthay MA.
Low tidal volume reduces epithelial and endothelial injury in acid-
injured rat lungs. *Am J Respir Crit Care Med* 2002;165:242–249.

19. Muscedere JG, Mullen JB, Gan K, Slutsky AS. Tidal ventilation at low
airway pressures can augment lung injury. *Am J Respir Crit Care Med*
1994;149:1327–1334.

20. Taskar V, John J, Evander E, Robertson B, Jonson B. Surfactant
dysfunction makes lungs vulnerable to repetitive collapse and reex-
pansion. *Am J Respir Crit Care Med* 1997;155:313–320.

21. Sinclair S, Molthen R, Haworth S, Waters C. Airway strain and tension
during mechanical ventilation in the intact rat [abstract]. *Am J Respir
Crit Care Med* 2006;3:A247.

22. Molthen R, Haworth S, Roerig D, Hanger C, Johnson R, Dawson C.
Cone-beam X-ray micro-computed tomography with concurrent
dynamic planar angiographic imaging and physiological measure-
ment. In: Proceedings of the conference on high resolution imaging
in small animals: instrumentation, applications and animal handling,
September 9–11, Rockville, MD, 2001.

23. Molthen RC, Karau KL, Dawson CA. Quantitative models of the rat
pulmonary arterial tree morphometry applied to hypoxia-induced arte-
rial remodeling. *J Appl Physiol* 2004;97:2372–2384. [Discussion, 2354.]

24. Powell WR. Static mechanical properties of the trachea and bronchial
tree. *J Biomech* 1975;8:111–117.

25. Green A, Adkins JA. Large elastic deformations and non-linear
continuum mechanics. London: Oxford University Press; 1960.

26. Phillips CG, Kaye SR, Schroter RC. A diameter-based reconstruction of
the branching pattern of the human bronchial tree. II. Mathematical
formulation. *Respir Physiol* 1994;98:219–226.

27. Raabe OG, Yeh HC, Schum GM, Phalen RF. Tracheobronchial geom-
etry: human, dog, rat and hamster. Albuquerque, NM: Lovelace Foun-
dation; 1976.

28. Koblinger L, Hofmann W. Stochastic morphological model of the rat
lung. *Anat Rec* 1988;221:533–539.

29. Phillips CG, Kaye SR. Diameter-based analysis of the branching geometry
of four mammalian bronchial trees. *Respir Physiol* 1995;102:303–316.

30. Tsuchida S, Engelberts D, Peltekova V, Hopkins N, Frndova H, Babyn
P, McKerlie C, Post M, McLoughlin P, Kavanagh BP. Atelectasis
causes alveolar injury in nonatelectatic lung regions. *Am J Respir Crit
Care Med* 2006;174:279–289.

31. Vawter DL, Matthews FL, West JB. Effect of shape and size of lung and
chest wall on stresses in the lung. *J Appl Physiol* 1975;39:9–17.

32. Hughes JM, Hoppin FG Jr, Mead J. Effect of lung inflation on bronchial
length and diameter in excised lungs. *J Appl Physiol* 1972;32:25–35.

33. Lambert RK. Sensitivity and specificity of the computational model for
maximal expiratory flow. *J Appl Physiol* 1984;57:958–970.

34. Lambert RK, Wilson TA, Hyatt RE, Rodarte JR. A computational
model for expiratory flow. *J Appl Physiol* 1982;52:44–56.

35. Naureckas ET, Dawson CA, Gerber BS, Gaver DP III, Gerber HL,
Linehan JH, Solway J, Samsel RW. Airway reopening pressure in
isolated rat lungs. *J Appl Physiol* 1994;76:1372–1377.

36. Brown RH, Herold C, Zerhouni EA, Mitzner W. Spontaneous airways
constrict during breath holding studied by high-resolution computed
tomography. *Chest* 1994;106:920–924.

37. Brown RH, Mitzner W. Effect of lung inflation and airway muscle tone
on airway diameter *in vivo*. *J Appl Physiol* 1996;80:1581–1588.

38. Brown RH, Mitzner W. Delayed distension of contracted airways with
lung inflation *in vivo*. *Am J Respir Crit Care Med* 2000;162:2113–2116.

39. Brown RH, Mitzner W. Airway closure with high PEEP *in vivo*. *J Appl
Physiol* 2000;89:956–960.

40. Lambert RK. Role of bronchial basement membrane in airway collapse.
J Appl Physiol 1991;71:666–673.

41. Tschumperlin DJ, Shively JD, Swartz MA, Silverman ES, Haley KJ,
Raab G, Drazen JM. Bronchial epithelial compression regulates
MAP kinase signaling and HB-EGF–like growth factor expression.
Am J Physiol Lung Cell Mol Physiol 2002;282:L904–L911.

42. Tschumperlin DJ, Margulies SS. Equibiaxial deformation–induced in-
jury of alveolar epithelial cells *in vitro*. *Am J Physiol* 1998;275:L1173–
L1183.

43. Carney D, DiRocco J, Nieman G. Dynamic alveolar mechanics and
ventilator-induced lung injury. *Crit Care Med* 2005;33:S122–S128.

44. DiRocco JD, Pavone LA, Carney DE, Lutz CJ, Gatto LA, Landas SK,
Nieman GF. Dynamic alveolar mechanics in four models of lung
injury. *Intensive Care Med* 2006;32:140–148.

45. Schiller HJ, McCann UG II, Carney DE, Gatto LA, Steinberg JM,
Nieman GF. Altered alveolar mechanics in the acutely injured lung.
Crit Care Med 2001;29:1049–1055.

46. Schiller HJ, Steinberg J, Halter J, McCann U, DaSilva M, Gatto LA,
Carney D, Nieman G. Alveolar inflation during generation of a quasi-
static pressure/volume curve in the acutely injured lung. *Crit Care
Med* 2003;31:1126–1133.

47. Gajic O, Lee J, Doerr CH, Berrios JC, Myers JL, Hubmayr RD.
Ventilator-induced cell wounding and repair in the intact lung. *Am
J Respir Crit Care Med* 2003;167:1057–1063.

48. Dreyfuss D, Saumon G. Ventilator-induced lung injury: lessons from
experimental studies. *Am J Respir Crit Care Med* 1998;157:294–323.

49. Carlton DP, Cummings JJ, Scheerer RG, Poulain FR, Bland RD. Lung
overexpansion increases pulmonary microvascular protein permeabil-
ity in young lambs. *J Appl Physiol* 1990;69:577–583.

50. Parker JC, Townsley MI, Rippe B, Taylor AE, Thigpen J. Increased
microvascular permeability in dog lungs due to high peak airway pres-
sures. *J Appl Physiol* 1984;57:1809–1816.

51. Noble PB, Turner DJ, Mitchell HW. Relationship of airway narrowing,
compliance, and cartilage in isolated bronchial segments. *J Appl Physiol*
2002;92:1119–1124.

52. Wagers S, Lundblad LK, Ekman M, Irvin CG, Bates JH. The allergic
mouse model of asthma: normal smooth muscle in an abnormal lung?
J Appl Physiol 2004;96:2019–2027.

53. Gillis HL, Lutchen KR. Airway remodeling in asthma amplifies hetero-
geneities in smooth muscle shortening causing hyperresponsiveness.
J Appl Physiol 1999;86:2001–2012.